

AirCargoChallenge 2022

Technical Report

Team #03

THUAIR(AIR)





清华大学

Tsinghua University

AIR CARGO CHALLENGE 2022



ACC 2022

Technical Report

Team Name: **THUAIR(AIR)**

Team Number: **No.3**

Team University: **Tsinghua University**

Finish Date: **2022-4-30**

Table of Contents

1	Introduction.....	3
1.1	Tsinghua University and THUAIR.....	3
1.2	Tsinghua University in Air Cargo Challenge.....	3
1.3	The Team of ACC2022.....	3
2	Project Management and Financial Budget.....	4
2.1	Financial Budget.....	4
2.2	Time Schedule.....	4
2.3	Sponsors and Supporters.....	5
3	Interpretation to Regulation and Principles.....	6
3.1	Review.....	6
3.2	New Rules.....	6
3.3	Size Calculation.....	6
3.4	Simulation Calculation.....	7
3.5	Takeoff and Climb.....	8
3.6	T Tail.....	11
3.7	Principles.....	11
4	Propulsion System.....	12
4.1	Static Thrust Test.....	12
4.2	Trust-Speed and Trust-Time.....	13
4.3	Turn Delta.....	13
4.4	The Influence of Fuselage.....	14
4.5	Push or Pull.....	14
5	Airfoil Design.....	17
5.1	Flap.....	17
5.2	Airfoil Optimization.....	19
6	Aerodynamic Design.....	21
6.1	Wing Span and Area.....	21
6.2	Dihedrals.....	21
6.3	Drag.....	22
6.4	Stability.....	23
6.5	Control.....	23
6.6	Verification Calculation.....	25
7	Structural Design.....	25
7.1	Main Wing.....	25
7.2	Cargo Bay and Fuselage.....	27
7.3	Tail Wing.....	28
7.4	Landing System.....	28
7.5	Weight Estimation.....	28
8	Payload Prediction.....	29
9	Conclusion and Outlook.....	29
10	Appendix.....	30

1. Introduction

1.1 Tsinghua University and THUAIR

Tsinghua University was established in 1911. As China's most renowned university, Tsinghua has become an important institution for scientific and engineering research.

Center of Aero Innovation & Realization for students (short for AIR) is an association of students affiliated to School of Aerospace Engineering of Tsinghua University. Since founded in 2007, our Center provides pleasant working-place and necessary equipment for both undergrad and graduate students to build and make our designs fly. We also have professors from School of Aerospace Engineering of Tsinghua University as consultants. Also, a club named THU Aeromodel was established in 2020 based on THUAIR, coming with a better management for our team.

1.2 Tsinghua University in Air Cargo Challenge

This is the 6th time that Tsinghua University to participate in Air Cargo Challenge, all of the team members participating before are from the organization AIR. In 2011, we participated ACC for the first time and win 3th place with more than 9kg payload carried. In 2013, we win 2nd place Portugal with 12.06kg payload. In 2015, we got 6th place in Stuttgart Germany. In 2017, a payload of 12 kg is our result and it was the 4th place. In 2019, we carried 10.82 kg payload to the sky and got 4th in the end. All of the participants have wonderful memories in ACC.



Figure 1. 1 Tsinghua University in ACC 2015, ACC2017 and ACC2019

1.3 The Team of ACC2022

The team with the same name with our organization consists of seven members.

Liu Xuan: 3rd year of bachelor course, major in Aerospace Engineering. Team leader and Team treasurer.

Huang Jian: 3rd year of bachelor course, major in Aerospace Engineering. Team management, preliminary design and aerodynamic design.

Yang Guici: Coach of AIR from 2008~2014. Pilot in ACC2011, ACC2013, ACC2017 and ACC2019. Main pilot in ACC2022.

Ning Bohao: 2rd year of bachelor course, major in Aerospace Engineering. CNC manufactory.

Tian Ganlan: 2rd year of bachelor course, major in Engineering Mechanics. Mold making for ACC2022.

Qian Shiyu: 2rd year of bachelor course, major in Aerospace Engineering. Drawing sheet making.

Ni Lichao: 2rd year of bachelor course, major in Engineering Mechanics. Model calculation.

Also there are 5 consultants guiding us all the time.

Ge Dongyun: associate professor of aircraft structure design. Adviser of the "AIR".

Chen Haixin: professor of aircraft aerodynamics design. Adviser of the "AIR".

Wei Wu: Engineer of structural strength design. The teacher in charge of AIR.

Shen Jingxiang: Member of AIR from 2012 to 2018.

Du Xuzhen: Member of AIR from 2011 to 2017.

2. Project management and financial budget

2.1 Financial Budget

Project cost form

Financial budget	Details	Expenses
Preparation	Power System	€1000
	Wing Mould	€3000
	Flight-test	€500
	Material	€800
	Others	€200
Competition		
	Airline tickets	Unknown
	Registration fee	€700
	Accommodation	Unknown
	Others	€200
Total		€6400+

2.2 Time Schedule

The time schedule is presented as following:

Task	Dec	Jan	Feb	Mar	Apr	May	Jun	Jul
------	-----	-----	-----	-----	-----	-----	-----	-----

Team formation								
Exploring material								
Testing Propulsion system								
CFD and airfoil design								
Test model								
Preliminary Report								
Test Flight								
Design Adjustment								
Technical Report								
Model Building								
Looking for sponsors								
Flight Test								
Pack Up								
Competition								

2.3 Sponsors and Supporters

Support from sponsors is vital for keeping this project going. During the preparation of this competition, School of Aerospace Engineering and Tsinghua University offered sufficient funds. Besides, the following sponsors and unit also provided reliable equipment and place.

Sponsors

KST

KST Digital Technology Limited offers good quality servos with comprehensive categories. Thanks to KST for offering us servos.



Haobo (Fujian) New Material Technology Co., Ltd.,

Haobo (Fujian) New Material Technology Co., Ltd., provides a complete R & D, manufacturing, marketing and technical support. The company regards HyboFOAM series high-performance PMI foam as the main product. Thanks to HaoboTechnology for offering us high-performance PMI foam.



Supporters

Hydrodynamics and wind tunnel lab of Tsinghua University. This lab is our neighbor, they have rich experience and reliable equipment for wind tunnel. We really appreciate that they helped us in testing thrust and airfoil.

3. Interpretation to regulation and conceptual design

3.1 Review

After ACC2015, introducing composite material technology is what THUAIR doing. In 2016, it made a breakthrough in composite technology and was successfully used in ACC 2017 and ACC 2019. In the past few years of use, we have explored the advantages of composite materials and the scope suitable for use. In the competition of ACC, which needs to take both speed and load into account, aircraft made by composite material has obvious advantages due to its high specific strength and almost zero deformation airfoil, which is reflected in the competition results of ACC 2017 and ACC 2019. This year, we will apply the composite technology on ACC 2022 without hesitating.

In ACC 2017 and ACC 2019, the aircraft of THUAIR team are all heavy-duty aircraft, and the take-off weight is almost the highest in the competition. However, due to the design aimed to have a high load and takeoff weight, it has a great disadvantage in flight distance in the same time (flight speed). Therefore, compared with the champion team, there is a big gap in flight speed.

3.2 New Rules

ACC 2022 enables almost completely different rules from ACC 2017 or ACC 2019. In order to advocate economy, smaller size and smaller propeller are inevitable. Also the new rules pay more attention to practicality, changing the past iron slab into a blood bag, which greatly increases the volume of the load. Therefore, it is necessary to design a complete streamlined fuselage instead of the carbon tube fuselage in the past ACC competition.

In the past ACC competitions, through the analysis of the dynamics and energy model of the aircraft during cruise and turning, the principle of blindly pursuing speed is not desirable. However, under the new regulations of ACC 2022, the flight mode and flight area have changed greatly. The contradiction in the turning process is no longer prominent, and the flight speed of the champion team of ACC 2019 was very fast. So we have to overturn the previous conclusion. This year, we hope to increase the cruise speed as much as possible and to ensure that the takeoff weight is not low at the same time.

3.3 Size Calculation

The rules stipulate that the whole aircraft shall be fully placed in the diamond frame

with the side length of 1.5m. The 1.5m diamond frame limits the configuration of the whole aircraft, which limits the maximum wingspan and the relationship between wingspan and tail force arm. Since the elevator deflection is required to provide sufficient lifting torque C_m during takeoff, and C_m is equal to the force F_l multiplied by the force arm L_w , we do not want to provide the lifting torque by providing excessive negative lift by the tail wing (which will reduce the maximum takeoff weight), so the tail force arm cannot be too small. At the same time, due to the manufacturing technology problem, we cannot avoid the tip stall problem by twisting the outer section of the wing, so the tip-root ratio must be strictly limited. according to our experience, it is conservatively estimated that the tip-root ratio should be more than 0.7. In addition, reducing the drag coefficient during level flight can reduce the induced drag as much as possible, and it is hoped that the aspect ratio shouldn't be less than 10. In order to ensure a sufficiently large aspect ratio, tail force arm and tip root ratio, the possible maximum wing area is about 0.55 m^2 .

3.4 Simulation Calculation

(Loading, unloading and prediction scores are not calculated.) After clarifying the size relationship, the simulation calculation is started by using some empirical data. According to many iterations, it is concluded that the estimation of the maximum load weight of 5kg and the total flight distance of 4000 meters is the most reasonable estimation. So we get the following curve.

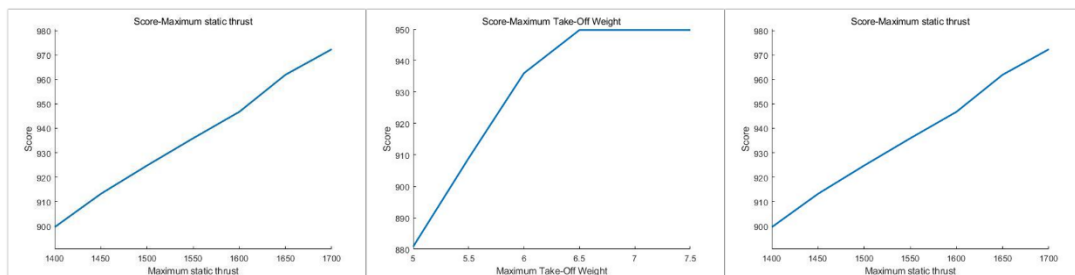


Figure 3.1 the effect of variables on score

The following characteristics are observed:

1. The influence of air density on load can not be ignored;
2. The effect of take-off bonus points is very significant for the results, so the plane should be pulled up within 40 meters;
3. Propeller thrust has a great influence on the final score, so we should make great efforts in the power system to find the most reasonable combination of blades, electric regulators and batteries;
4. When the take-off bonus points can be obtained and the wing area is within $0.45\text{-}0.55 \text{ m}^2$ and weight of take-off is in the range of 6-7 kg, the difference of final score is no more than 5%, and this 5% gap can be easily erased in production and flying.

Therefore, more consideration should be taken into manufacturing and flying. At the same time, in order to ensure the take-off bonus points, some allowance should be left in the actual load when flying.

3.5 Takeoff and Climb

takeoff and sliding:

In the analysis, we believe that it is very important to be able to pull up the aircraft within 40 meters, so the takeoff and taxiing process is worth studying in detail.

The dynamics model of take-off and taxiway is a simple variable acceleration problem. According to Newton Second Law we have:

$$m \frac{dv}{dt} = T(v) - D(v)$$

Here, thrust is calculated in the previous section as battery is fully charged (12.3V). And the drag force consists of several terms, which remain to be calculated separately. The friction of the ground disappears gradually with the increase of lift:

$$D_{friction} = \mu \left(mg - \frac{1}{2} \rho v^2 A_{wing} CL_{rolling} \right)$$

Aerodynamic drag can be divided into the sum of the contributions of wings, fuselage, tail and landing gear. However, it is worth emphasizing that due to the ground effect, the induced drag felt by the wing here is far less than the value in free space and should be estimated separately. Here, a trapezoidal wing is selected, whose airfoil is 2021_OPT16m2, with a wingspan of 2.2m, wing area range of 0.35-0.7m², shoot-root ratio of 0.6 and flaps of 9°. The Angle of attack is 2.5° (running state, Cl =1.56). We use the ground effect model of XFLR5 (the ground height is 12cm) to calculate the aerodynamic drag of main wing within the range of 1~12 m/s. And the results obtained can be well fitted as:

$$D_{wing} = (0.06v + 0.013v^2) \cdot A_{wing}^{1.1}$$

The unit of velocity is m/s, the unit of wing area A_{wing} is m², and the unit of drag is N.

Obviously, the larger the wing area, the larger the tail area required. Assuming that the flat tail capacity is 0.4 and the tail moment arm length is 0.5m, we have:

$$0.4 = \frac{A_{tail} \cdot 0.5m}{A_{wing} \cdot MAC}$$

In which aerodynamic chord length:

$$MAC = \frac{0.98 \cdot A_{wing}}{2.2m}$$

So we get:

$$\frac{A_{tail}}{A_{wing}} = \frac{A_{wing}}{2.806m^2}$$

Flat tail is a symmetrical airfoil, and the drag coefficient is about half of the airfoil. But this is only the flat tail considered, so we have to add another 50% roughly to the drag on account of the vertical tail. When considering tail drag, the drag is equivalent to multiplying main wing drag by a factor.

$$D_{wing+tail} = (0.06v + 0.013v^2) \cdot A_{wing} \cdot \left(1 + \frac{0.75A_{wing}}{2.806m^2}\right)$$

The body drag is estimated according to the streamline body, which is approximately (discussed in 4.6)

$$D_{fuselage} = 0.003 \cdot v^2$$

Here we assume that retractable landing gear is used and the gear drag is not temporarily considered.

The logic of the takeoff procedure is as follows.

For a given take-off weight, wing area, lift coefficient at the moment of take-off, Take-off speed v_t is given directly by the lift formula. The running distance is obtained by integrating the variable acceleration motion.

$$s = \int v dt = \int_0^{v_t} \frac{mvdv}{T(v) - D(v)}$$

Climbing:

Similarly, in our analysis, we believe that among all the teams, there must be a team that can get a full score for climbing. Whether we can climb to 100 meters within the specified time greatly affects the final score, so the climbing process must be calculated.

After offsetting various drag forces, the remaining thrust allows the aircraft to climb.

The induced drag:

$$D_i = \frac{1}{2} \rho v^2 A_{wing} \cdot \frac{CL^2}{\pi Span^2 / A_{wing}} = \frac{2Lift^2}{\pi Span^2 \rho v^2}$$

Airfoil drag plus tail drag:

$$D_{foil} = \frac{Lift}{80} \cdot \left(1 + \frac{0.75A_{wing}}{2.806m^2}\right)$$

Airframe drag:

$$D_{fuselage} = 0.003 \cdot v^2$$

Rate of climb:

$$r = v \cdot \frac{T(v) - D(v)}{mg}$$

It is easy to imagine that if the velocity is too low, the induced drag will be too significant. And on the other hand, if you go too fast, the drag of the airfoil and fuselage is too great, which means you could have the maximum rate of climb only at an optimal speed. The speed in the climbing stage is the speed corresponding to the maximum climbing rate. For this year's race, the optimal rate of climb is about 15~17m/s, corresponding to $CL \approx 1$.

The thrust in the climbing stage is the result of average of full electric thrust and medium electric thrust. The maximum height that can be climbed in a period of time (say 60 seconds) is the optimal rate of climb multiplied by the climb duration.

However, the takeoff speed is less than this optimal climb speed, so a horizontal acceleration stage is required before the climb begins. It is easy to imagine that this is the most dangerous time, when a sudden gust of wind coming or a mistaken manipulation could easily damage the plane. The length of this time can easily be found from the equation of variable acceleration. Obviously, this acceleration time increases as takeoff weight increases. We can also see the significance of introducing the criterion of "residual thrust factor θ " in the calculation of take-off state. This criterion effectively limits the length of this acceleration time.

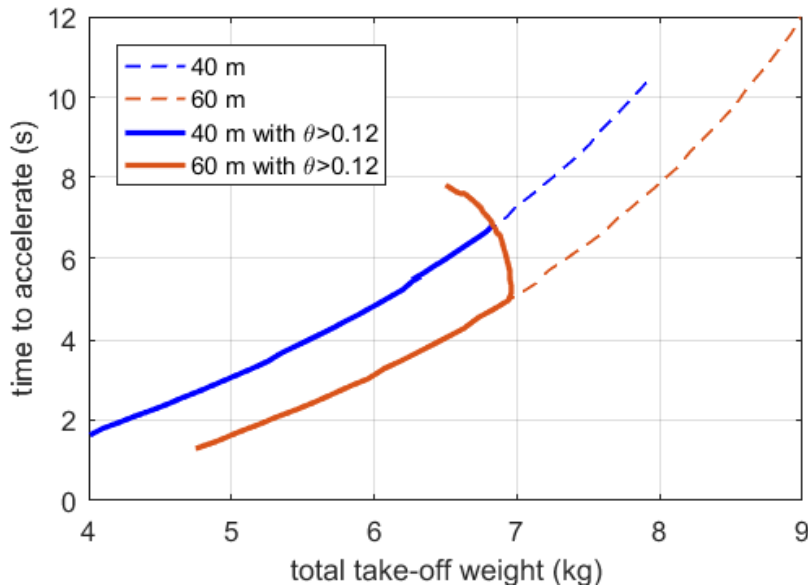


Figure 3.2

So, the real time available for climbing is actually 60 seconds minus this acceleration time. In order to allow some margin, five seconds were deducted from this. The final score for the climb is also divided by the team with the highest score. Considering certainly by that kind of flying speed party, certainly by climbing points close to full marks. So the climb points can also be calculated.

3.6 T Tail

When analyzing the aircraft in the previous ACC teams with good results, it is easy to find that many of them use T-tail or V-tail. In the ACC2022 project, we also hope to do some research on the tails.

Due to the limitation of the size of the diamond frame, the tail has to be installed close to the main wing, which means that the conventional tails will be in a strong downwash flow of the main wing, or even in turbulent flow. At the same time, due to the interference of the huge fuselage, the incoming flow of the tails is very chaotic and unpredictable. In this case, the conventional tail is not a wise choice.

Under many considerations, we have to make an attempt. This will be the first time for us to design and manufacture the T-tail. In the test plane before the formal one, the wooden T-tail performs well (figure 3.2), and the structural strength also meets our requirement. Therefore, we finally decided to bring the T-tail to ACC2022.



Figure 3.3 Wooden T-tail without rudder surface

At the same time, the deep stall problem that may exist in the T-tail itself must be weakened or avoided in other ways, such as increasing the static stability margin or increasing the elevator area.

3.7 Principles

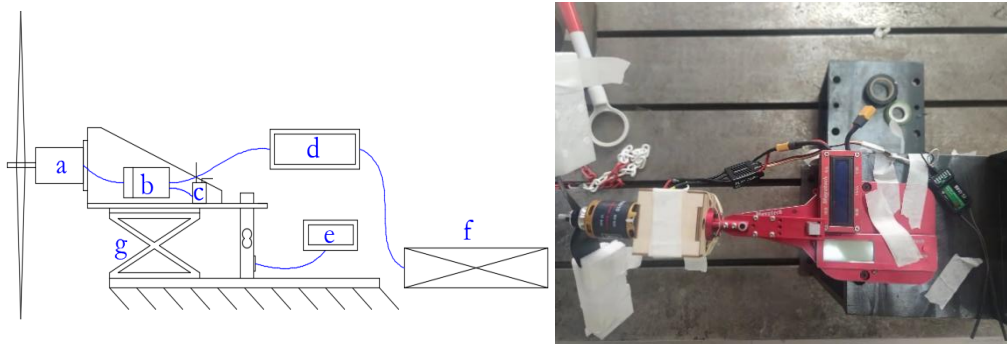
For ACC2022, the load and wing area can be placed in a reasonable range, and there is little difference in the final score within this range. In contrast, whether you can take off within 40 meters so as to get bonus points and how to match the power system to fully release the power are the keys to this competition. In addition, because the aircraft of ACC2022 is smaller and the influence of details is enlarged, we hope to

handle the details of the aircraft better and make the aircraft close to our design as much as possible.

4 Propulsion System

4.1 Static Thrust Test

In order to select the most suitable battery and accurately know the parameters of the motor and propeller used in the competition, we have built a test platform as shown in the figure below, including a test platform, a set of force measuring devices, data display instrument, ammeter, motor mounting base, motor with propeller, receiver, electric regulator, remote controller, etc., which are installed, connected and calibrated.



a: motor b: ESC c: receiver d: ammeter e: digital display f: battery g: measuring device
figure 4.1

According to previous experience, the old and new motors have little impact on the static thrust, while the type of battery will have a greater impact. Therefore, we tested four different batteries. The figure below shows the thrust data with four different batteries. According to the thrust data, we have selected the battery.

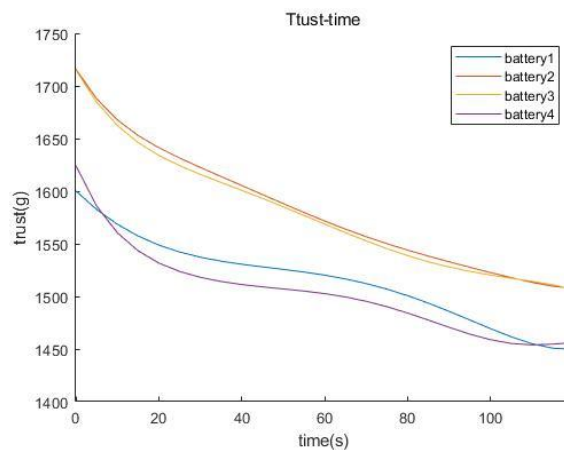


figure 4.2

4.2 Trust-Speed and Time

The battery 3 above was used to test the dynamic thrust in a wind tunnel, and the change of thrust with time under the wind speed of 5m/s, 10 m/s, 15 m/s, 20 m/s and 25 m/s was tested. Due to the slow speed when taking off and climbing, battery discharges with the high voltage and short time, we estimated that the thrust in the take-off stage was a stable number. The change of the stable thrust with the wind speed is shown below.

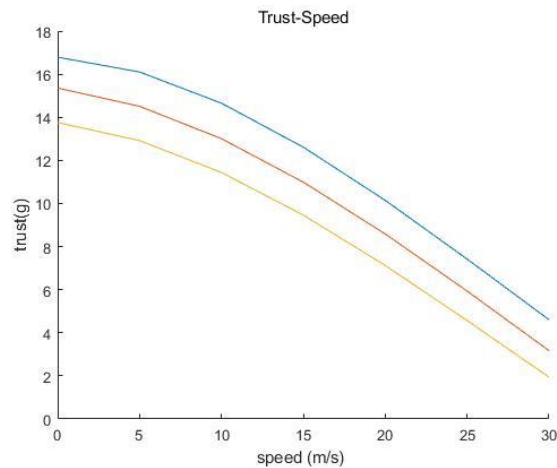


Figure 4.3

4.3 Turn Delta

As for the turn delta, the above test platform is still used. By adjusting the turn delta of the ESC through the multifunction LCD program box, the data measured are shown as follows:

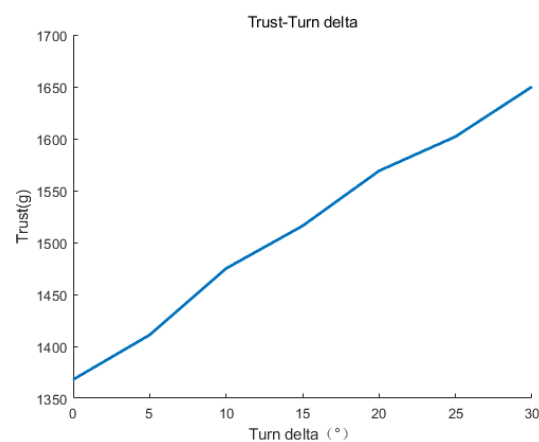


Figure 4.4

We can clearly see that the larger the delta, the greater the thrust, so the turn delta of 30° was chose .

4.4 the influence of fuselage

There is slipstream effect in fixed wing aircraft, which is a decrease of effective thrust caused by the drag of fuselage in propeller slipstream. In addition, with the turbulence taken by the rotation of propeller, the influence of fuselage could be not negligible. So the drag brought by fuselage reduces the propulsion efficiency of the system. This effect is less obvious near the center line of propeller because the fuselage is located in the area where the propeller inflow is slow. The blocking effect depends on the blocking coefficient B .

It is defined as $B = \frac{D_{fus}}{D}$ where D_{fus} is the maximum area of the fuselage and D is the area of the propeller. For general aviation propeller, it is suggested that when the blockage rate is lower than the critical value, the fuselage blockage can be ignored. The estimated value of critical plugging rate is between 0.33 and 0.42. For every 10% increase in the blockage rate above the critical value, the efficiency will be reduced by 1%, and the typical reduction is about 5%, which is due to the slipstream effect of light general aviation aircraft with tractor configuration. For a small UAV, this effect is expected to be more obvious due to the significant reduction of Reynolds numbers of propeller and fuselage. As for our design, the $D_{fus} = 15000 \text{ mm}^2$ and $D = 50000 \text{ mm}^2$, so the calculated B is about 0.3. According to this study, its impact on the plane is negligible.

4.5 Push or pull

If the motor and propeller are placed at the end of fuselage (called push below), it is possible to maintain laminar flow in the front fuselage (about in front of the wing). In the following, the drag of laminar flow and turbulent fuselage is estimated respectively, and then linear interpolation is made as the estimation of fuselage drag of push.

The fuselage is estimated to be a streamline body with a diameter of about 140mm and a total length of 1m. Volume Reynolds number:

$$R_{ev} = \frac{10^5}{1.5} \cdot V^{\frac{1}{3}}(m) \cdot v(m/s)$$

Through a study (<http://dx.doi.org/10.1155/2014/470715>), for a streamline body with good shape, if the fuselage surface is full laminar flow or full turbulence, the volume drag coefficient is about:

$$Cd_{V-lam} \approx \frac{4.708}{(R_{ev})^{\frac{1}{2}}} \quad Cd_{V-turb} \approx \frac{0.435}{(R_{ev})^{1/5}}$$

At 12, 17 and 27 m/s, it is about $Re_v = 1.66e5$, $2.36e5$ and $3.74e5$. The relationship between volume drag coefficient and drag is

$$D = \frac{1}{2} \rho v^2 C_{d_v} V^{2/3}$$

The drag estimation given by it is basically consistent with a more serious article after multiplying by 1.2 (<https://doi.org/10.2514/6.1997-1483>) Therefore, the fuselage drag coefficient estimation formula adopted here is:

$$C_{d_{V-lam}} \approx \frac{5.65}{(Re_v)^{\frac{1}{2}}} \quad C_{d_{V-turb}} \approx \frac{0.52}{(Re_v)^{\frac{1}{5}}} \quad D = \frac{1}{2} \rho v^2 C_{d_v} V^{2/3}$$

Under the volume Reynolds numbers corresponding to 12, 17 and 27 m / s, the corresponding volume drag coefficients of 40% laminar flow are:

	12 m/s; $Re_v=1.66e5$	17 m/s; $Re_v=2.36e5$	27 m/s; $Re_v=3.74e5$
40% laminar flow C_{d_v}	0.0337	0.0309	0.0277
40% laminar flow drag(N)	0.128	0.236	0.532
40% laminar flow γ	0.00089	0.00082	0.00073

40% laminar flow corresponds to the actual condition of the backward motor.

The fuselage of the pull is completely immersed in the propeller slipstream. In addition to the fact that the fuselage is obviously full turbulence, additional drag will be generated due to the fact that the slipstream velocity of the propeller is greater than the airspeed.

First, the propeller slipstream velocity is estimated. According to the propeller momentum theory, the propeller disc area is a ($0.05m^2$), the incoming flow velocity is V_0 , and if the slip flow velocity is $V_0 + v_s$, the thrust is

$$T = \rho v_s (v_0 + v_s/2) A$$

Therefore, the slipstream velocity can be pushed back by the thrust at each airspeed. During takeoff (12 m / s full power), climb (17 m / s 50% full + 50% medium power) and cruise (27 m / s medium power), the slipstream speed is:

	Incoming flow velocity (m/s)	Thrust (N)	Slip flow velocity $V_0 + v_s$ (m/s)	Slip flow /Incoming flow
Takeoff	12	12.54 N	23.53 m/s	1.96
Climb	17	9.80	24.68	1.45
Cruise	27	4.36	29.52	1.09

According to the above approximate formula of total turbulence, the fuselage drag can be estimated as follows:

Airspeed	12 m/s	17 m/s	27 m/s
Slip flow velocity	23.53 m/s	24.68 m/s	29.52 m/s

Fuselage Re_V (e5)	3.263	3.422	4.093
Cd_{v-turb}	0.0410	0.0407	0.0392
Drag (N)	0.600	0.654	0.902
γ	0.0042	0.0023	0.0012

Note that, by definition, here γ is the total drag divided by the square of airspeed (not slipstream velocity). As an estimate in the previous section, take $\gamma = 0.003$ corresponds to the situation here.

Then to calculate separately for takeoff, climb and cruise. γ Value is substituted into the program in the previous section to obtain the comparison results of pull (blue) and push (red). It can be found that the advantage of push is not obvious.

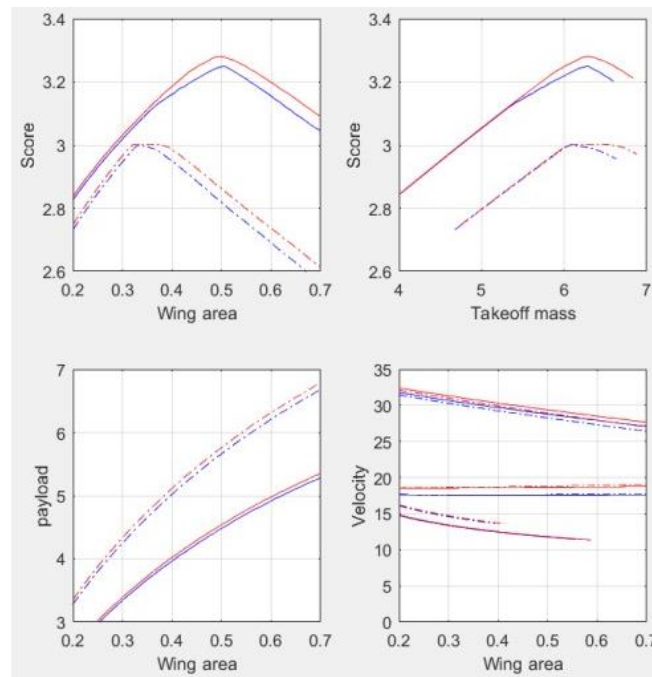


Figure 4.5

Although in principle, the push can obtain a faster maximum speed with less fuselage drag (fuselage drag is not significant in takeoff and climb compared with wing drag), so it can achieve the same score at a smaller payload. However, the results here show that when the take-off weight is about 6kg, the dominant response is only about 150g on the payload (the final score of push of 4.2kg payload is the same as that of pull of 4.35kg payload). Therefore, push has no advantages over pull, especially considering that there will be various problems in push in actual operation:

- 1) In order to prevent the propeller from hitting the ground, it needs a very high landing gear and ventral fins;
- 2) The motor cannot be installed too far back, so the tail force arm is shorter and requires a larger tail area;
- 3) It will reduce the voltage drop between the motor and the battery, because it is necessary to arrange some long wires. For example, considering that the distance

between the motor and the battery is increased by 30 cm, an additional 60 cm conductor is added. According to the calculation of 3mm diameter aluminum wire, the resistance of 60-cm wire is about 2.4 milliohm. At 28A current, it brings about a voltage drop of about 0.07v, which corresponds to about 13g thrust. This little perturbation should not affect the takeoff thrust weight ratio, so it corresponds to reducing 60g takeoff weight. Considering that the dead weight of conductor is about 12g, the total effect is equivalent to reducing 72g load. While the pull has only a disadvantage of about 150g in total, this means a half decrease.

So, finally we decide to use the conventional layout of motor and propeller to ensure reliability.

5. Airfoil Design

5.1 Flap

The results of our analysis show that the requirements for airfoil are summarized as follows:

- 1) excellent lift-drag ratio during takeoff and climb
- 2) The ratio of lift coefficient in take-off to drag coefficient in cruise shall be as large as possible. (The lift coefficient in cruise state shall be approximately 1 / 4 of that in takeoff state)

Using flaps is a classic solution. Of course, the Fowler flap can definitely perform better. But in fact, when preparing for acc2015 in the spring of 2015, we found that the slide rail mechanism is not only complex to make, but also the problem of self-locking can hardly be avoided after taking off because of the air drag and vibration.

Meanwhile, it is necessary for flap to make full use of the whole wingspan. If the flaps are only arranged in the middle section, on the one hand, the area of the airfoil with high lift coefficient is not enough; on the other hand, the lift distribution in the take-off state is closer to the "bell distribution"; the wing without flaps in the outer section is just only equivalent to put winglet flat, and the lift drag ratio is obviously not as good as the elliptical distribution under the same span. Therefore, the outermost flap also plays the role of aileron, which eliminates a large number of flap forms that can only deflect downward and cannot deflect upward.

In our estimation program, the dependence on the airfoil is only reflected in three aspects: lift coefficient when taking off (about 80% of the maximum lift coefficient), climb-drag ratio (taken as 80) and drag coefficient when cruising(0.0075).

For example, fuller flaps can greatly improve the maximum lift coefficient (from about

1.8 to about 2.8), so as to improve the take-off lift coefficient (from 1.45 to 2.2) and reduce the wing area. However, the climb-drag ratio and cruising drag coefficient are likely to decrease.

To compare the performance of the two, which is shown below, the takeoff lift coefficient is changed from 1.45 (blue) to 2.2 (red).

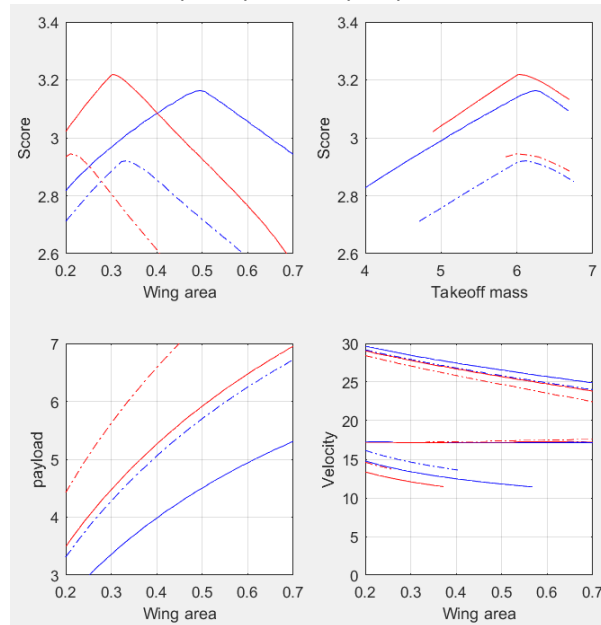


Figure 5.1

the dotted line is 60m running distance, which can be ignored

It can be found that the use of slotted flaps can reduce the wing area from 0.45 m² to 0.31 m², reducing the empty weight of wings with about 150g, which also increases the payload of about 200g and slightly improve the maximum speed.

Considering that there is no ready-made scheme for flap slide rail or other mechanism, CFD for analyzing slotted airfoil is not as simple and reliable as Xfoil. and because the Reynolds number of the wing is smaller after reducing the wing area, it seems unwise to add so many uncertainties for these non decisive advantages.

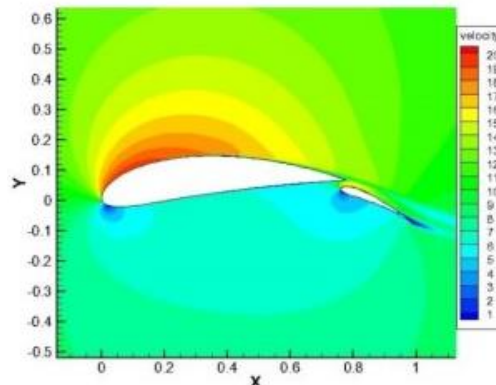


Figure 5.2 (slotted flaps in ACC2017)

5.2 Airfoil Optimization

Based on the constraints of climb rate and take-off distance, the optimal load capacity, wing area and the speed of take-off, climb and cruise are estimated. We abandoned the high lift airfoil in ACC2015 and 2017 and chose the optimized airfoil based on opt16. Combined with the smaller wing and thinner thickness of the aircraft of ACC2022, it is difficult to arrange complex backward flaps or multi end flaps, so we chose the concept of simple flap and made appropriate fine adjustment based on the opt16 airfoil optimized by ACC2019 (the thickness was reduced to 10.7 and the streamline was scrambled at 55% on the upper surface), and a new generation of opt16m2 was obtained. These fine adjustments are mainly to adapt to the lower Reynolds number of ACC2022. The simple flap hinge is located at 74%.

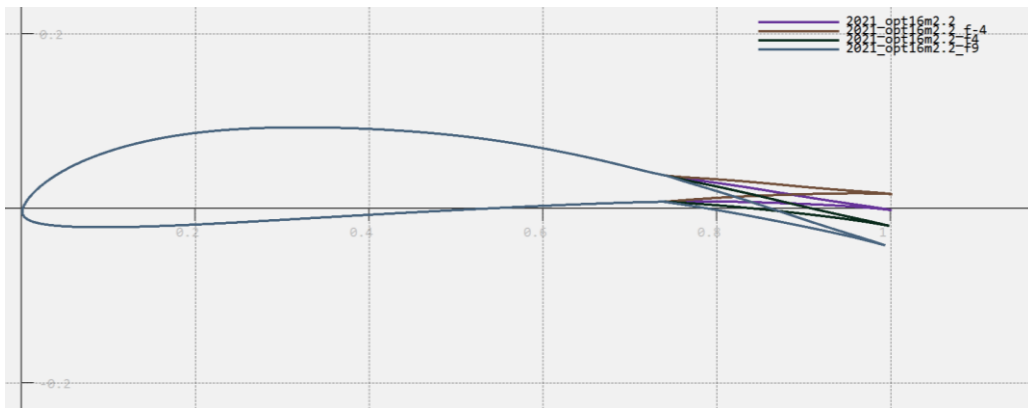


Figure 5.3

Here, the calculation condition of $Re * \sqrt{CL} = 241000$ is selected, which corresponds to aspect ratio = 10 and total weight = 6.5kg. When the flap deflection angles are - 4°, 0°, 4° and 9°, the lift coefficient and lift drag ratio are:

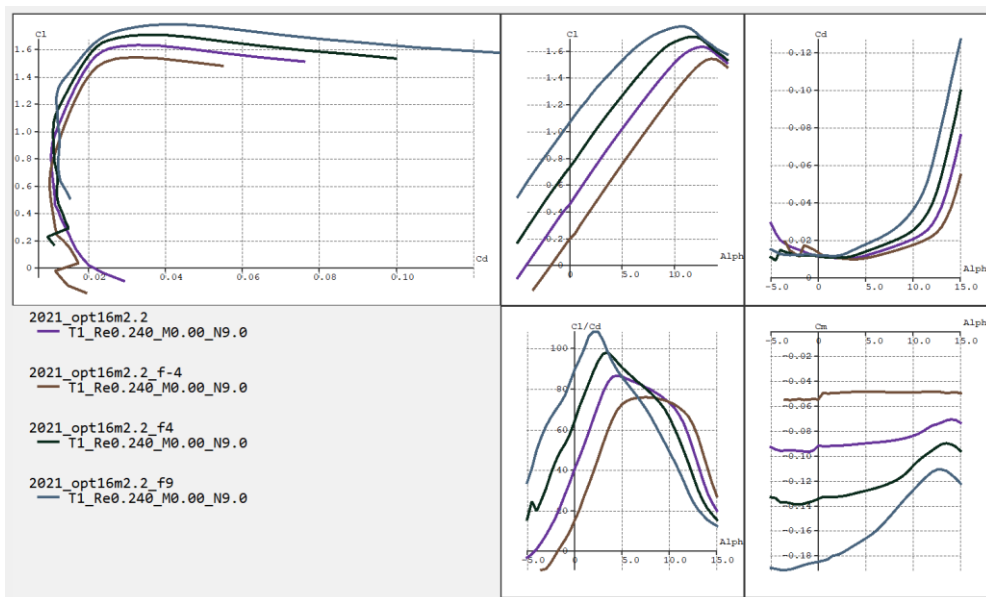


Figure 5.4

But as we can see from the figure, the thickness of 2021_opt16m2.2 airfoil at 74% is only 2.8%, the average chord length in the preliminary design is about 20-25cm, and the thickness at the flap position is too thin to be processed.

Therefore, based on this, we thickened the 2021_opt16m2.2 airfoil at 74% to obtain 2021_opt16m2.3. According to the characteristics of 2021_opt16m2.3, we slightly modified the flap angle and selected the flap deflection angle of 10° during takeoff.

The maximum lift coefficient given by 10° flap deflection angle is about 1.8, and the available lift coefficient at the moment of takeoff is about 1.45. The minimum lift coefficient (before stall on the lower surface) allowed by the flap deflection angle of 4° is about 0.3.

In the climbing stage, it is considered that the lift-drag ratio of the airfoil = 80 is a reasonable estimation, because the lift coefficient in the climbing state can always fall into the "high lift drag ratio pocket" by adjusting the flap deflection angle within a certain range. We use Xflr5 software to analyze and get the optimal angle of the climbing flap, which is 2° . At 2° , we can get the maximum lift coefficient of 1.35 when the lift drag ratio is greater than 80.

However, when approaching the maximum speed (i.e., $CL \approx 0.3$), the drag coefficient remains stable regardless of the change of the flap deflection angle, which is approximately 0.0072. Based on the lift line position, a more appropriate flap angle (-4 degrees) is selected. This drag coefficient is close to the limit, while the other wing scheme (2021_mh32m1.1), which makes a large concession on the maximum lift coefficient, has a minimum drag coefficient of 0.0065 when $CL=0.3$.

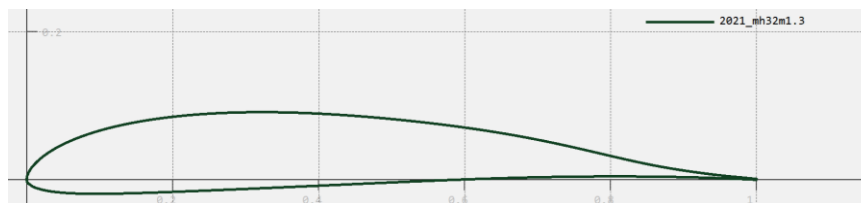


Figure 5.5

Finally, we got the final airfoil and its three working states - 2021_opt16m2.3_f10, 2021_opt16m2.3_f2, and 2021_opt16m2.3_f-4 as follows.

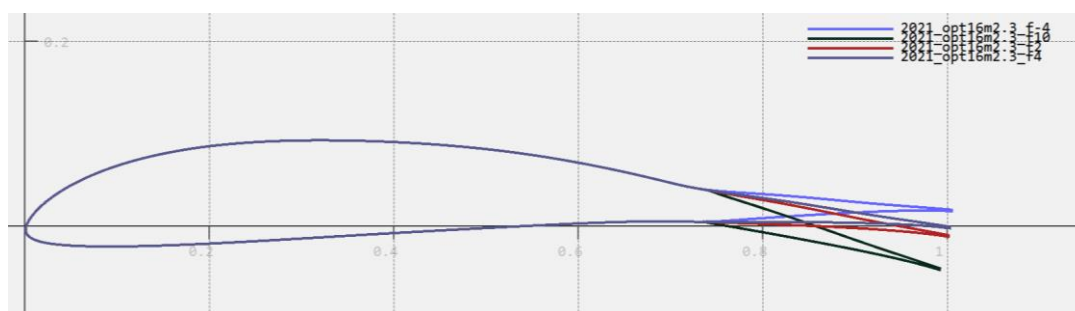


Figure 5.6

6 Aerodynamic Design

6.1 Wing span and area

Based on the previous discussion, we chose the general layout. According to the conclusion in 3.4, we set the maximum take-off weight at 6.4 kg and the wing area at 0.49 square meters. In order to maximize the aspect ratio as well as combine the setting of the taper ratio more than 0.7, we set the following wing parameters: wing span 2.2 meters, root chord length 260mm, tip chord length 190mm. As set above, we calculated the lift distribution of the wing in xflr5.

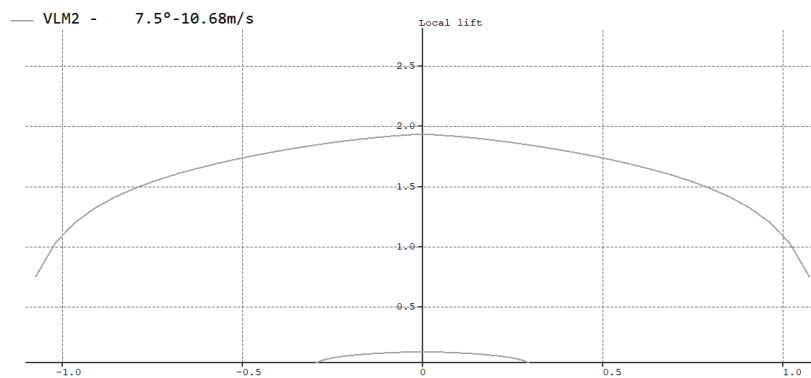


Figure 6.1 lift distribution at take-off

It's not hard to see from the figures that the lift distribution is not perfect. In order to further improve the climbing lift-drag ratio, reduce the induced drag and do not affect the drag coefficient when cruising, we decided to add an 80mm high miniature symmetrical airfoil to the wing. The calculation results show that the winglet only reduce the lift-drag ratio by less than 1% when flying flat, but increase the lift-drag ratio by 7% when climbing and taking off, which is very effective. At the same time, the winglet not only hardly increases the root bending moment and roll damping, but also increases the aileron rudder efficiency to a certain extent, which is a good design.

6.2 Dihedral

For takeoff and climb, we want to keep the ailerons as little as possible. This is mainly because: 1. This state has low speed, poor aileron rudder efficiency, and the airfoil works near the stall angle of attack. Deflecting the ailerons at this point, it may create a sharp point on the wing surface to induce separation and destroy the monolithic airfoil. 2. If the rudder does not cooperate with the ailerons, the low speed due to asymmetric induced drag and airfoil drag will cause a large anti-yaw torque, which may further cause counter control of the ailerons. For the above reasons, we designed the climb phase according to the unmoved ailerons situation. So this is going to mean that we need to have enough roll stability. And an important factor affecting roll stability

exactly is the dihedral. The larger the dihedral, the stronger the roll stability. However, the dihedral should not be too large, otherwise it will affect the ailerons turning in high speed mode. Based on past design experience, 2° dihedral with a slightly swept-back wing and a upper vertical tail are sufficient for roll stability. Also it doesn't make the roll too damped.

6.3 Drag

Fuselage drag coefficient:

We cite the calculation method of fuselage drag coefficient on the website http://www.dept.aoe.vt.edu/~mason/Mason_f/MRsoft.html#codemenu .by using it, we give the correlation between drag coefficient and Reynolds number. For the wall friction coefficient of streamlined fuselage, the following empirical formula is given

$$FF = 1.0 + 1.5 \left(\frac{d}{l} \right)^{1.5} + 50 \left(\frac{d}{l} \right)^3$$

d is the maximum diameter and l is the length of fuselage

For the whole aircraft, the problem of fuselage drag coefficient during cruise is more prominent. So we focus on the drag coefficient on cruising. Assuming that the aircraft travels at 25m/s. We introduced aircraft data into the site's calculations, and get the fuselage drag coefficient is 0.0032. We can see this value is in good agreement with the drag coefficient we estimate before (4.5). Compared with previous carbon tube fuselage, which fuselage drag coefficient is 0.001, there is a large increment.

Drag coefficient of lift surface:

During flat flight, the drag coefficient between the wings and the tail is 0.011. At takeoff, the drag coefficient is 0.092. When climbing, the drag coefficient is 0.054.

Parasite drag:

Estimation: we follow the methods used to estimate the ACC2017 again:

Component	γ_{part}	Number	γ	Remarks
Servo connecting rod	0.000271	6	0.000735	
Fuselage	0.0032	1	0.0032	Given above
Vertical tail	0.00166	1	0.00166	Xflr5: HT12 60% Rudder surface is tilted 5°
Main landing gear	0.0002	2	0.0004	Streamline
Main lifting wheel	0.00033	2	0.00066	
Front landing gear	0.001	1	0.001	

Total			0.00766	
-------	--	--	---------	--

Based on the above analysis, the parasite drag is close to the drag coefficient of the lift surface during cruise. Therefore, we are more determined in the details and engineering of the reduction of drag.

6.4 Stability

Pitching stability:

In order to ensure sufficient tail capacity (more than 0.4) and tail arm (more than 0.45m) at the same time, finally the tail arm and the flat tail area are determined. Also we get 0.45 tail capacity. Xflr5 analysis can be seen: With take-off climb speed, static stability margin is 16%. In high-speed mode, the static stability margin is 4.5%. It can ensure enough stability in the climbing stage, and it can be sensitive enough after the speed adds up.

Since the longitudinal stability of conventional layout is generally not a major problem, we will not overstate it.

Course stability:

Due to the size limitation of the diamond frame, the tail arm is short. And there is part of the vertical tail in the wake of the fuselage. So the vertical tail is less efficient. At the same time, too large and too long fuselage has side effects on course stability, which cannot be estimated. In summary, we cannot predict the course stability of our aircraft precisely. To be on the safe side, we will make the vertical tail larger and add the end plate to the outer end of the flat tail.

6.5 Manipulation

Pitch control:

Generally, the range of elevator is 20%-30% of the tail area, but due to the strict size limitation of ACC2022, the tail moment arm is short, and we used T tail, so we increased the elevator area for fear that the aircraft would be difficult to change when entering a deep stall.

Yaw control:

Similar to longitudinal maneuvering, we chose a larger rudder area because of the shorter moment arm and potentially weaker directional stability.

Roll control:

Assuming that the wingspan is b , and the length of the flap is b_0 . So the roll moment generated by the aileron will be:

$$\tau = \frac{b - b_0}{2} \frac{\rho v^2 S}{2} \delta Cl \frac{b_0}{b}$$

δCl : the difference between the lift coefficient of maximum positive deflection and maximum negative deflection of aileron.

The aerodynamic damping of the roll direction is defined as the reverse roll moment generated by the roll Angle w . We assume that the slope of the lift line at each section is $2\pi/\text{rad}$.

$$\gamma = \frac{2}{\omega} \int_0^{\frac{b}{2}} x \cdot \frac{\rho v^2 S}{2} \cdot 2\pi \frac{\omega x}{v} \cdot \frac{dx}{b} = \frac{\pi}{12} \rho v S b^2$$

For composite wings, the wing weight is approximately proportional to the area, and the proportional coefficient is σ . Therefore, the moment of inertia in the rolling direction is:

$$I = \frac{m_{wing} b^2}{12} = \frac{\sigma S b^2}{12}$$

So the equation of motion can be reduced to:

$$\ddot{\theta} = \frac{3\rho v^2 \delta Cl}{\sigma} \cdot \frac{(b - b_0)b_0}{b^3} - \frac{\pi\rho v}{\sigma} \dot{\theta}$$

Using initial value conditions, the ordinary differential equation can be solved as follows:

$$\theta = \frac{3v\delta Cl}{\pi} \frac{(b - b_0)b_0}{b^3} \left(t - \frac{\sigma}{\pi\rho v} e^{-\frac{\pi\rho v}{\sigma} t} \right)$$

The time constant $\tau = \frac{\sigma}{\pi\rho v} = 0.01317$ is so small that the exponential term can be omitted when calculating the time at $\theta = \pi/3$.

Define $b = 2.2, v = 25\text{m/s}, \delta Cl = 1.2, \sigma = 1.2\text{kg/m}^2, \rho = 1.16\text{kg/m}^3$ to calculate and to observe the relationship between b_0 and time.

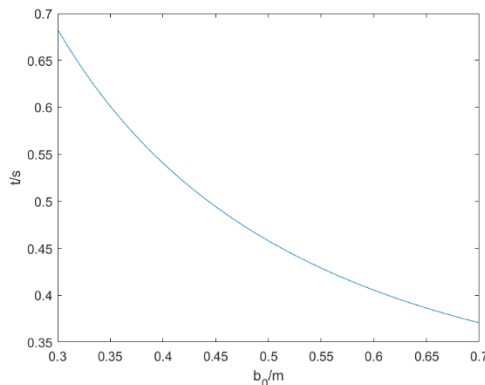


Figure 6.2

Due to the dihedral of the wing, to ensure sufficient rolling moment, we set the 500mm (0.23 times wingspan) length of the wing as flaperon and the inner section as flaps.

6.6 Verification Calculation

Takeoff distance:

Set C_l as 1.5, m as 6.4 kg, density as 1.16, friction resistance as 0.04 and wing area as 0.495 m^2 . Based on 3.5 and combined thrust curve, we could get the distance of takeoff is 36.1m, which is less than 38m. There should be enough margin to take off within 40 m, because it is necessary to take something into account such as directional correction and possible wing rubbing.

Rate of climb:

Use xflr5 to model and calculate wing drag and turn down the flap, with 0 degrees Angle of attack of the whole plane. Using the Drag calculated by 6.3 and combined with thrust curve, climb rates at different speeds can be calculated.

The dimensionless parameter describing the climb rate is 9.2%, which also meets the request that more than 8%.

7. Structural Design

7.1 Main Wing

Skin part:

The composite technology with good effect in previous years is adopted. The lay-up of the wing shells is shown in the figure. The carbon wave clothed at the leading edge and the main beam form a D-box, which bears almost all the torque and bending moment on the main wing. $10\text{g}/\text{m}^2$ carbon felt is used as the outermost layer because of its light weight and rich glue in the finished product. And because of not fully mastered the painting process and lack of equipment, we think the black glue rich surface formed by carbon felt is more convenient for later treatment. In addition, the main wing sandwich also includes 1mmPMI foam and 1 layers of fiberglass cloth.

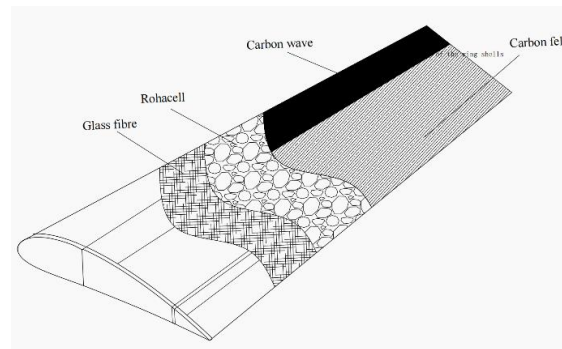


figure 7.1

Beam part:

The main beam is set at the position of 34% chord length, and the position of 34% chord length of each section of the wing is on the same plane, which is convenient for manufacturing. Due to the size limitation of the laser cutting machine, we divide the main beam into two sections, each 1025mm. Since the beam is mainly subjected to bending moment, in order to have sufficient capacity to bear bending moment, the wood grain direction must be perpendicular to the long axis. So several boards are bonded together and wood chips are used to ensure that the material was completely dense. At the same time, carbon strips and Kevlar are used to strengthen the main beam to ensure the strength of the main beam.

Because we used composite technology to build our aircraft, the mold is essential. Our main wing mold is made of 5166 Epoxy Tooling board. In addition, in order to save cost and make it simple, 460 Epoxy Tooling board are used in the flat tail and vertical tail mold, and nylon plates are used in the wheel mold.

Wing-Fuselage: A sufficiently strong carbon-betula composite plate is buried inside the fuselage as a central wing beam, extends to both sides and is inserted into the box beam at the wing root. At the same time, two bolts are used to connect the wing rib plate and the fuselage side wall to ensure that it will not fall off and can withstand a certain bending moment.



Main wing

Wheel

Figure 7.2

7.2 Cargo Bay and Fuselage

According to the load design mentioned above and reserving a certain space, the layout of four section cargo bay is chosen. (figure 7.3)

The first section: cargo bay 1, which can place a battery (red marked part) and two 300g + two 200g water bags or three 300g water bags.

The second section: cargo bay 2, which can place four 300g water bags.

The third section: cargo bay 3, which can place automated measurement equipment (red marked part) and four 300g water bags.

The fourth section: cargo bay 4, which can place three 300g water bags

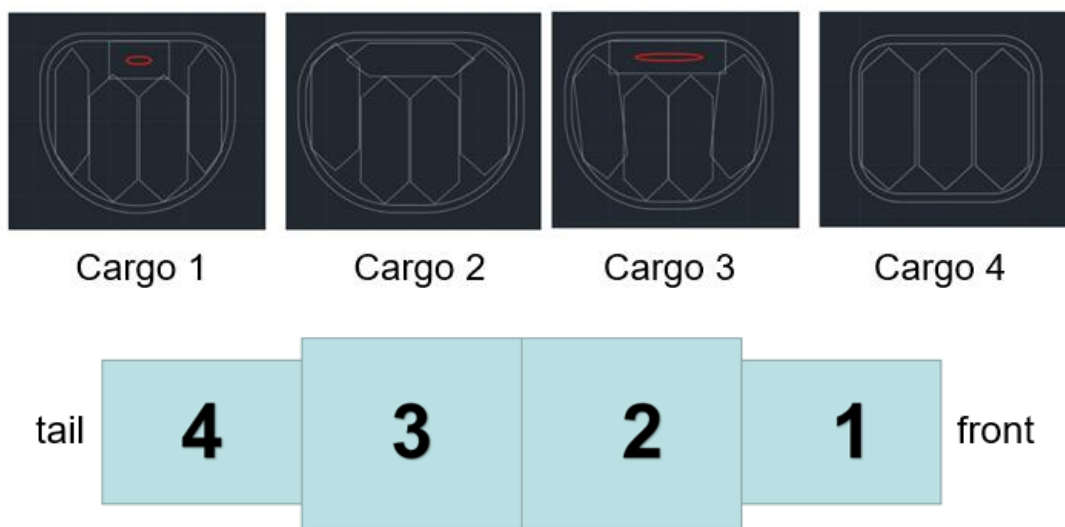


Figure 7.3

According to the above cargo bay section design, the fuselage with similar to streamlined low drag can be gotten through SolidWorks lofting as follows:

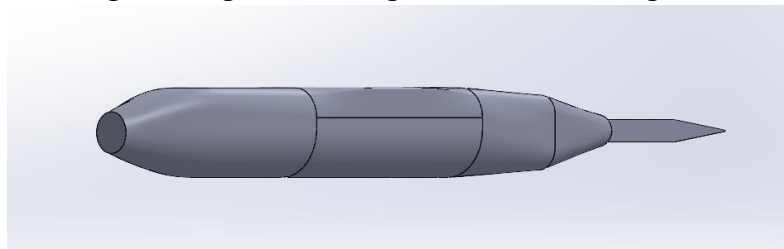


Figure 7.4

Since the fuselage of acc2022 needs to transmit torque, tension, lift and load, composite materials are still used to make the fuselage to ensure strength, stiffness and minimize weight. In order to ensure sufficient tensile strength and bending stiffness, LV cloth with high tensile strength is used as the matrix, resin is used as the adhesive to ensure the stiffness, supplemented by carbon wire as the reinforcing rib, and a reinforcing frame is set inside to ensure the strength of the opening.

7.3 Tail Wing

Since we adopted the T-shaped tail for the first time, we have no experience in its structural strength for reference. In order to ensure sufficient structural strength, the stiffness and modulus of the vertical tail need to be large enough, composite materials are still used. For the convenience of the connection between the flat tail and the vertical tail, the lower surface of the flat tail and the upper surface of the vertical tail have been modified to increase the contact area, and the bolt connection is used on the contact surface. The two blue faces in the figure are connecting faces.

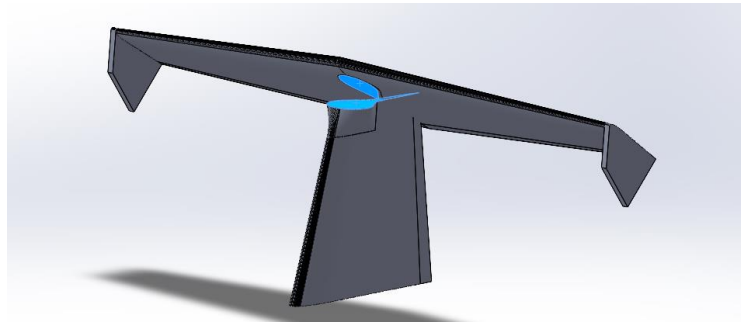


figure 7.5

7.4 Landing system

In order to ensure a large enough take-off angle, we have to increase the height of the main landing gear. In order to ensure sufficient stiffness and cushioning capacity, the landing gear support made of carbon fiber are chosen. To further reduce the weight, the wheels made of carbon fiber cloth and balsa core are chosen, which performed well in ACC2017 and 19. The wheels are connected to the landing gear in the position marked in the figure with carbon tubes and bearings.

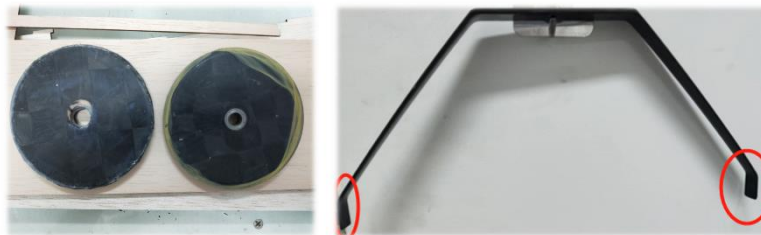


figure 7.6

7.5 Weight Estimation

Weight Estimation of Each part(g)	
wing	550
Power system	600

Landing gear	200
Empennage	150
Servos and cables	100
Fuselage and cargo bay	600
Total	2200

8. Payload prediction

In the research before, it is more important for the plane to take off within 38 meters with a margin of 5% for the pilot. The relationship between load(kg) and air density(kg/m^3) can be summarized as follows:

$$m(\rho)_{\text{payload}} = 2.9 \times \rho + 1.003$$

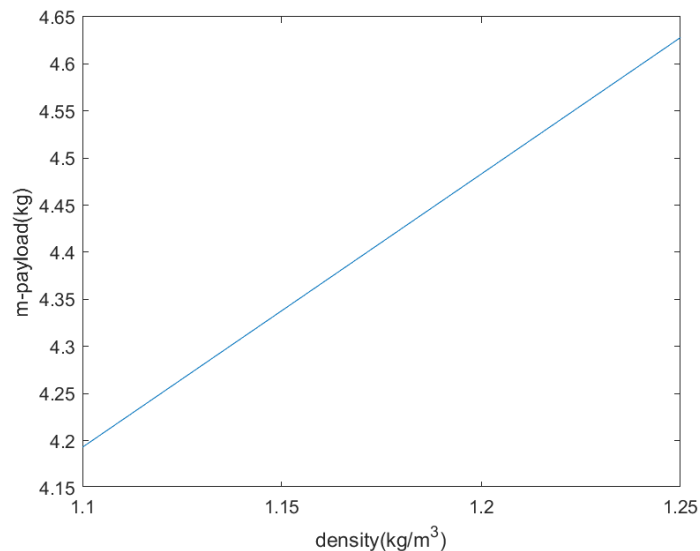


figure 8.1

9. Conclusion and Outlook

After about six months of hard work, now we move forward to this important timing point-handing in the Report. We feel pleased about what we have done, but at the same time we also know that we still have a lot of work to do in the next two months. During the process of preparing ACC 2022, all of our team members have achieved a lot of knowledge which can or can't be found in books. Besides, all the team members build a strong friendship in this project. We all appreciate the opportunity of participating in this competition.

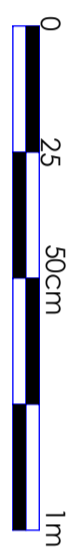
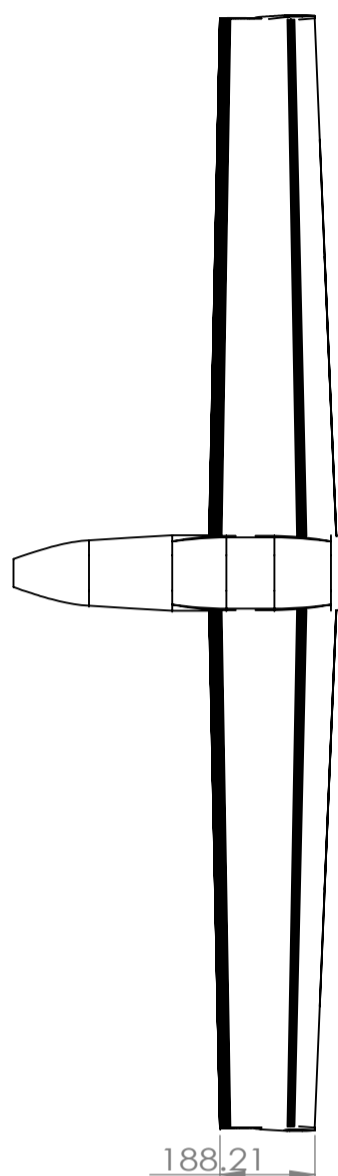
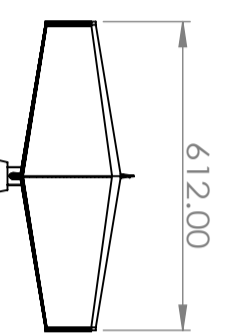
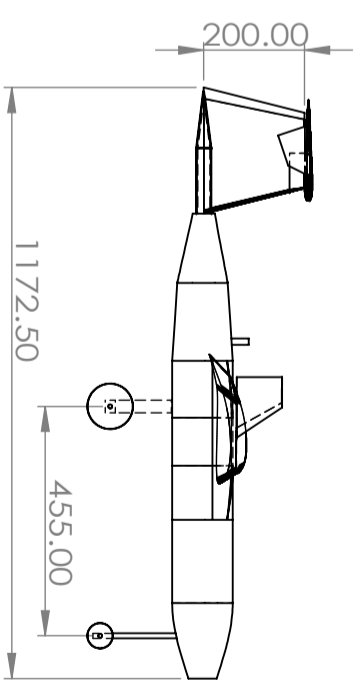
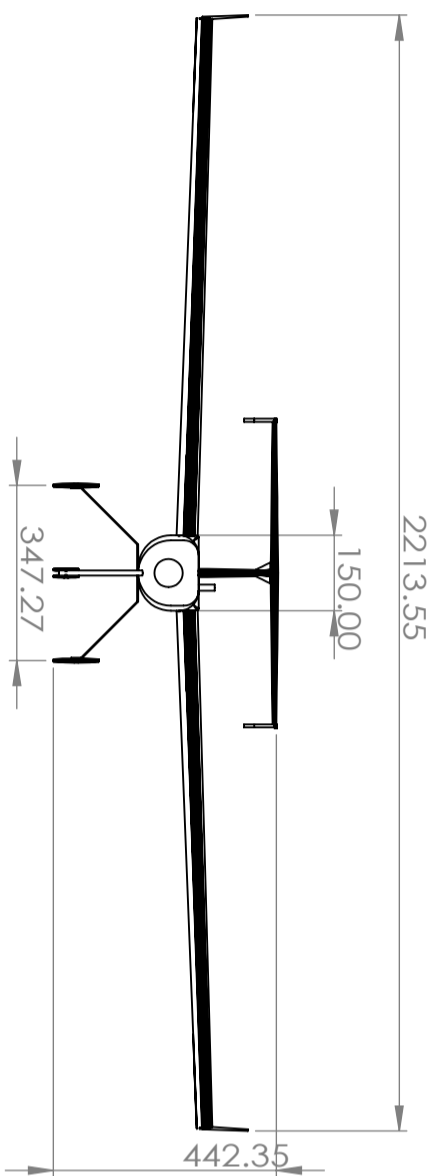
10. Appendix

3-view drawing

Isometric perspective view

Cargo bay

Lay-up of the wing shells



Detail Size Information of The Aircraft

Wing Span	2213.55mm
Wing Area	0.495m ²
Length of Tail Moment Arm	480mm
Fuselage Length	635mm
Root Chord	260mm
Tip Chord	190mm
Tip-Root Ratio	0.73
Aspect Ratio	10
Sweep Angle	21°
Horizontal Tail Area	0.09m ²
Vertical Tail Area	0.04m ²
Tread	347.3mm
Wheelbase	455mm
Volume of Cargo Bay	0.009m ³

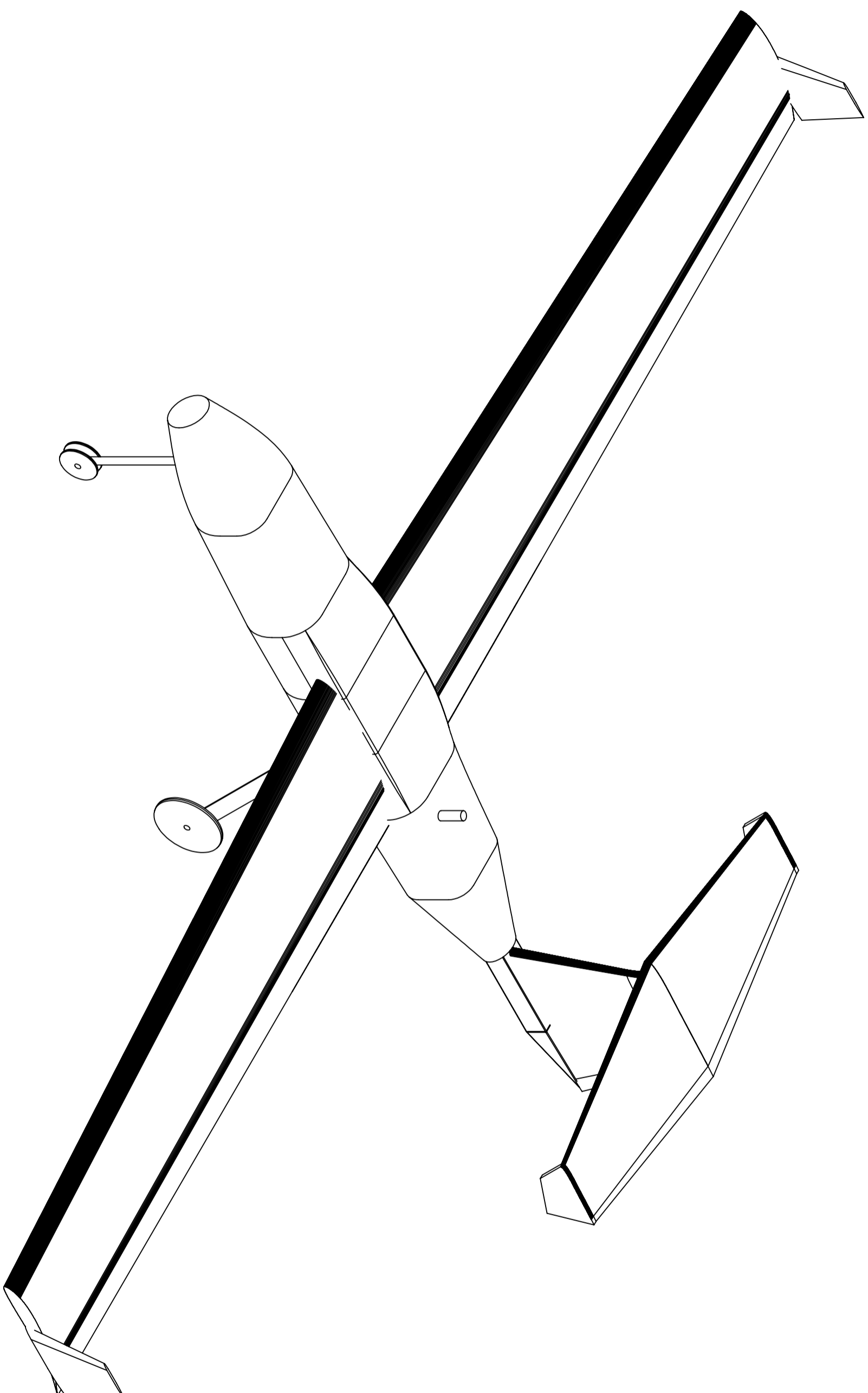
Air Cargo Challenge 2022
 Team Number: No.3
 Team Name: THUAIR



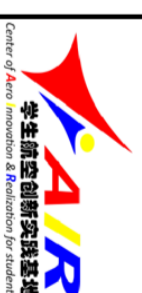
Scale:1/15

Isometric Drawing

page:1/4



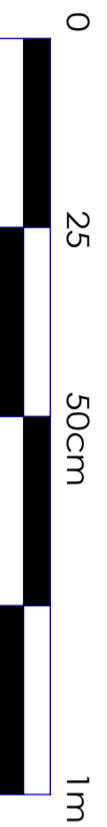
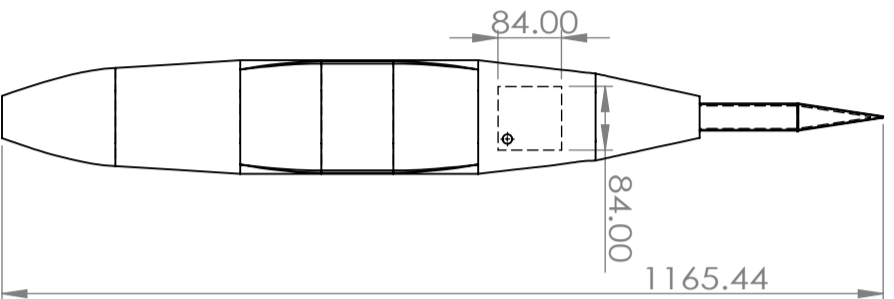
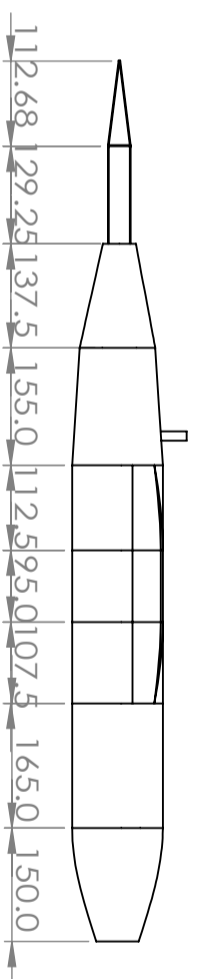
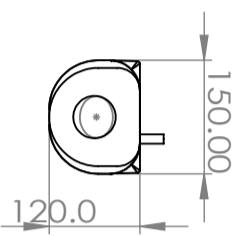
Air Cargo Challenge 2022
Team Number: No.3
Team Name: THUAIR






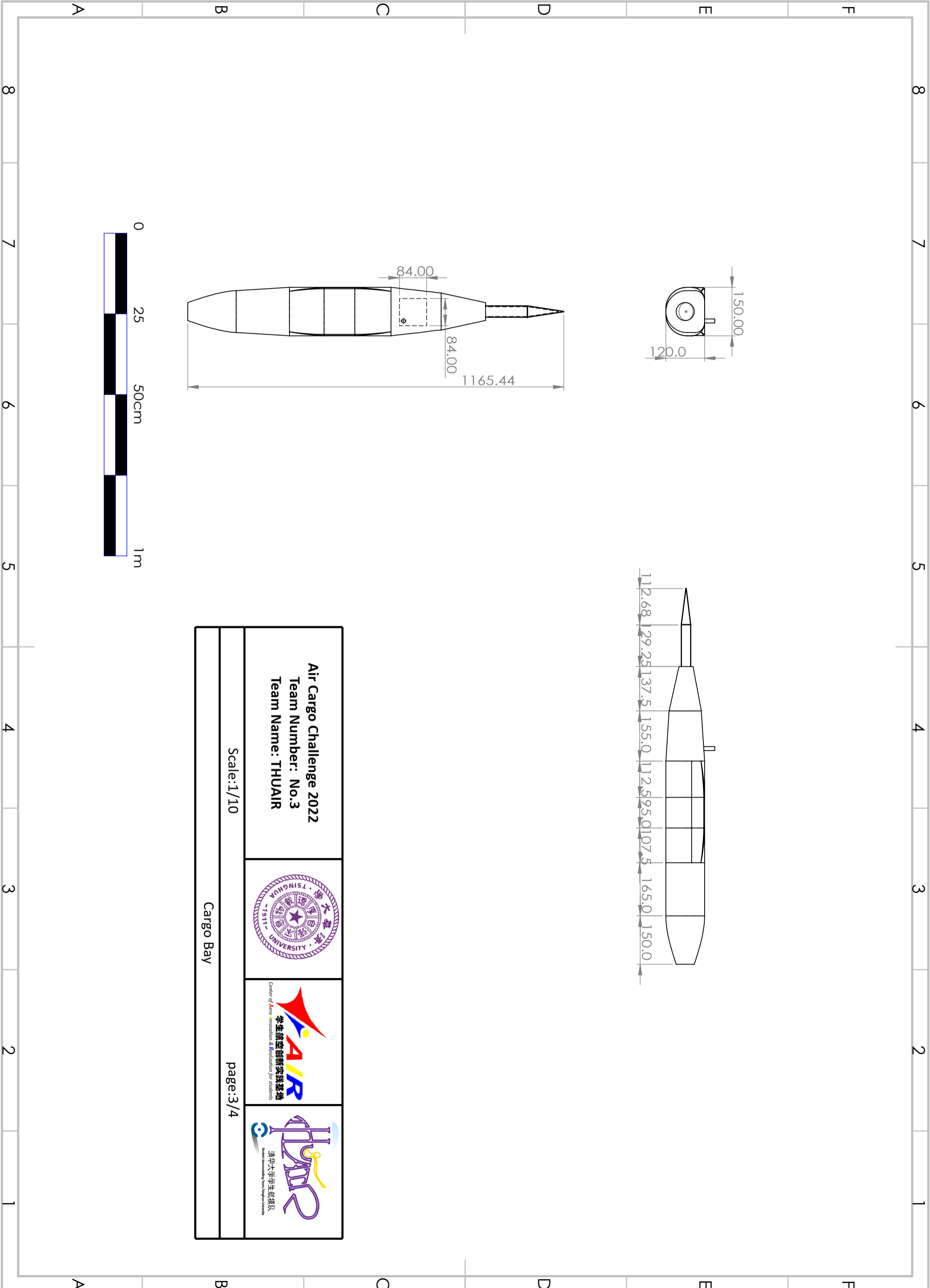
Scale:1/5

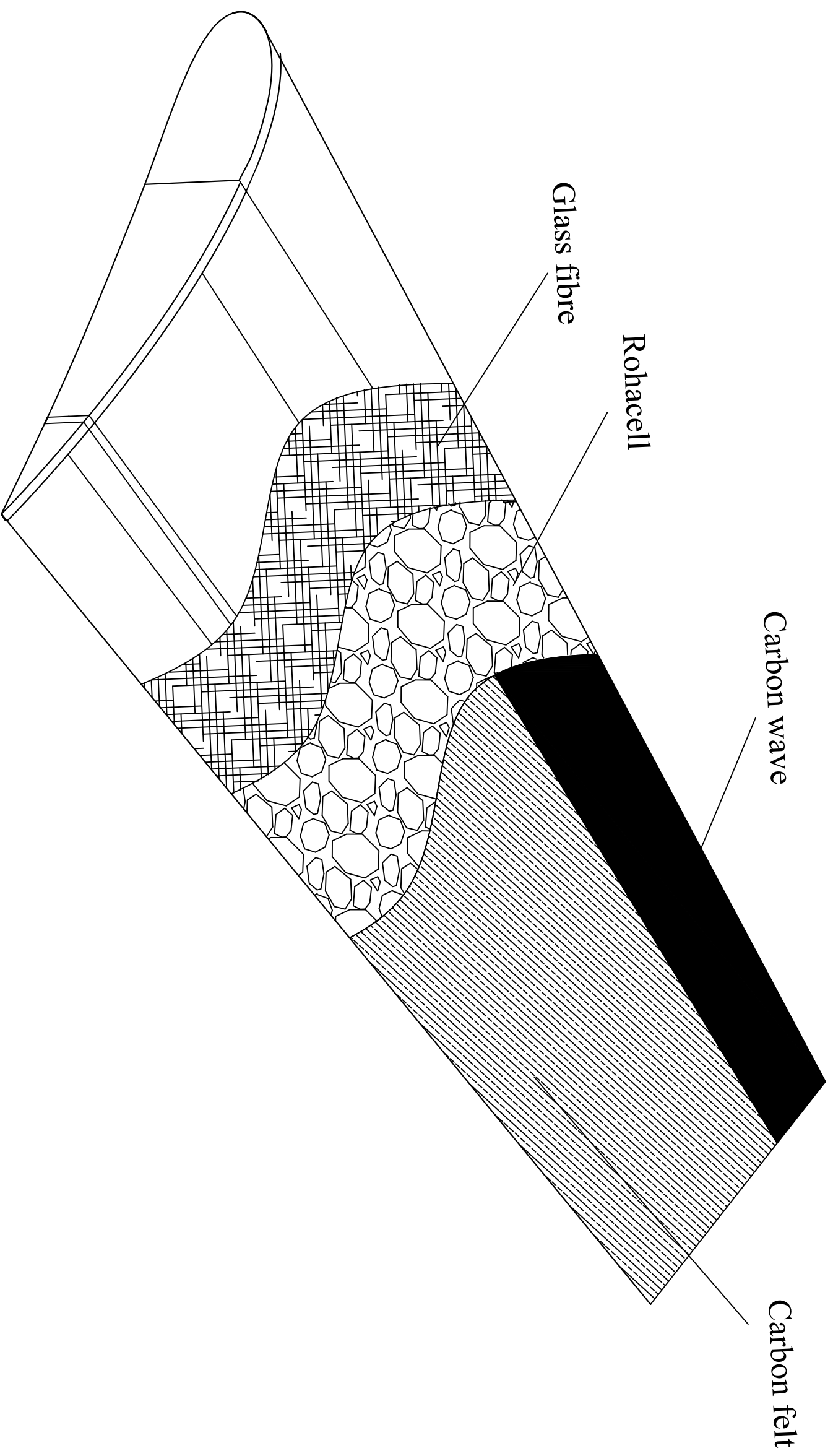
page:2/4




Isometric Drawing



Air Cargo Challenge 2022 Team Number: No.3 Team Name: THUAIR			
Scale:1/10	Cargo Bay		
page:3/4			





<p>Air Cargo Challenge 2022 Team Number: No.3 Team Name: THUAIR</p>			
<p>Scale:1/1.5</p>		<p>page:4/4</p>	
<p>Lay-up of the wing shells</p>			